# RADIATION THERMOMETRY - THE MEASUREMENT PROBLEM*

G.D. Nutter

Instrumentation Systems Center

University of Wisconsin - Madison

* Based on a paper by the same title published in "Applications of Radiation Thermometry," ASTM STP 895, 1985.

# RADIATION THERMOMETRY - THE MEASUREMENT PROBLEM

## INTRODUCTION

Radiation thermometry is the measurement of the temperature of an object by radiometric methods. A radiation thermometer is a radiometer calibrated to indicate the temperature of a blackbody having the same apparent radiance as the "target, the specific surface area over which the temperature is to be measured. An idealized radiation thermometer is illustrated in Fig. 1.

This method of temperature measurement is used when contact with the heated object - such as by a thermocouple - is undesirable or impossible, e.g., when the target is in motion, is inaccessible or would be damaged by contact, when the target temperature might be perturbed by a contact device, or when the target temperature is so high that the intense heat would degrade or destroy a contact temperature sensor. Radiometric methods are particularly important in industrial processes and in laboratory applications.

Radiation thermometry can be separated into three parts: the radiator (the target), the environment between the target and the radiation thermometer, and the radiation thermometer

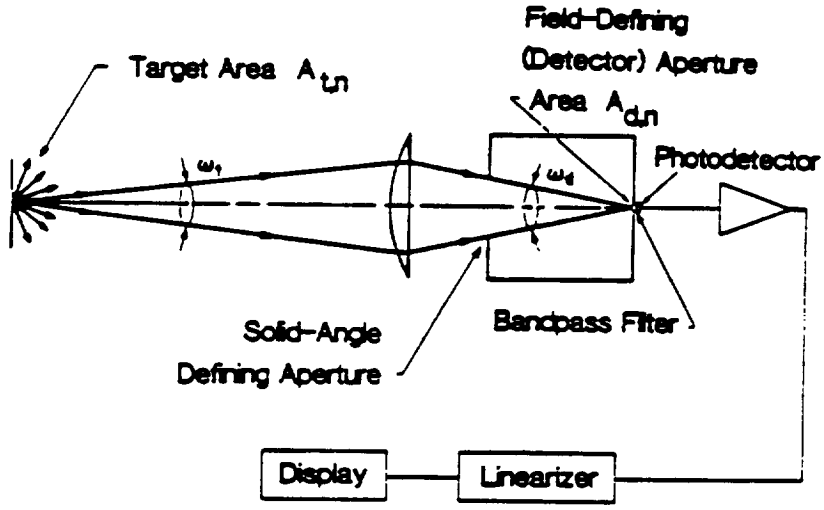


Fig. 1. Idealized Radiation Thermometer
The radiometer output signal is directly proportional to spectral radiance, which is exponentially related to temperature through Planck's radiation law.

itself. We begin by considering blackbody radiation, which forms the theoretical basis for radiation thermometry.

## THERMAL RADIATORS

### BLACKBODIES

A blackbody is a surface that absorbs all electromagnetic radiation incident on it, reflecting nothing. At room temperature, such a surface would appear to be absolutely black, but at sufficiently elevated temperatures it would glow somewhat more brightly than the surface of any real material at the same temperature. The spectral radiance of a blackbody is given as a function of temperature $T$ and wavelength $\lambda$ by the Planck radiation distribution (Fig. 2):

$$L_{\lambda,b}(\lambda,T) = \frac{c_1}{\lambda^5 \cdot (e^{c_2/\lambda \cdot T} - 1)} \qquad (1)$$

where

$$c_1 = 2 \cdot c^2 \cdot h = 1.191062 \times 10^8 \ [W \cdot \mu m^4 \cdot sr^{-1} \cdot m^{-2}] \ ; \qquad (2)$$

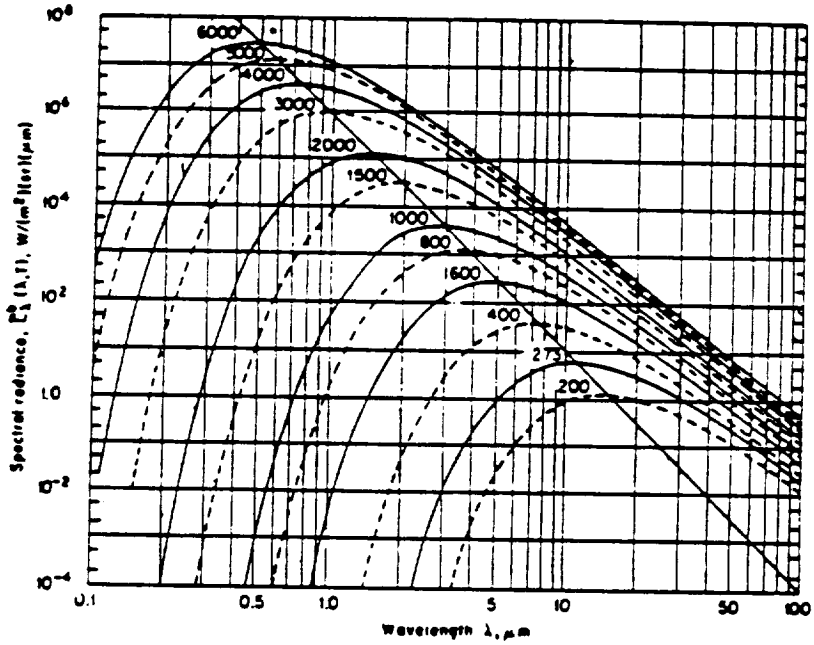


Fig. 2. Spectral radiance of a blackbody, from Planck's radiation law. Temperature in kelvins is shown for each curve.

$$c_2 = c \cdot h/k = 1.438786 \times 10^4 \ [\mu m \cdot K] \ ; \qquad (3)$$

$c$ is the velocity of light ;

$h$ is Planck's constant ;

$k$ is the Boltzmann constant

The spectral radiance of a surface (Fig. 3) is defined as

$$L_\lambda(\lambda) = \frac{\partial^3 \Phi(\lambda)}{\partial A \cdot \cos\theta \cdot \partial\omega \cdot \partial\lambda} \qquad (4)$$

where $\partial^3\Phi(\lambda)$ is the electromagnetic radiant flux (watts) in the spectral band $\partial\lambda$ at wavelength $\lambda$ radiating into the elemental solid angle $\partial\omega$ from the elemental area $\partial A$ having its normal at an angle $\theta$ with the elemental beam. The spectral radiance of a surface can be recognized as corresponding closely to the quantity perceived by the eye as brightness, and has the very important property of being invariant along a ray. This invariance is the basis for the usefulness of spectral radiance in radiometry

A blackbody surface is, strictly speaking, a purely hypothetical entity. No such material surface exists in practice, but blackbody radiation does exist. An opaque isothermal cavity is filled with blackbody radiation characteristic of

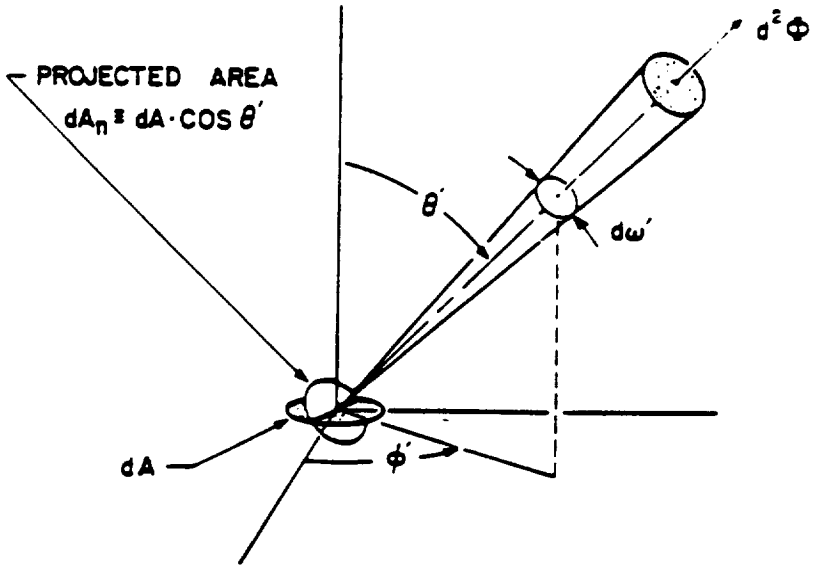


Fig. 3. Geometric aspects of spectral radiance, defined to be the derivative of radiance with respect to wavelength.

the temperature of the cavity wall; such radiation is isotropic and "unpolarized." If a small aperture is made through the wall, the escaping radiation very closely approximates that of a blackbody. Because of the invariance of the spectral radiance along a ray, the spectral radiance of the aperture is equal to that of the inner wall of the blackbody opposite the aperture as viewed along the ray. Such cavity radiators have long been used to simulate blackbodies experimentally and can be made to do so with high accuracy. This provides the experimental basis for calibrating a radiometer in terms of blackbody temperature.

## NON-BLACKBODIES

All real materials at temperatures above absolute zero also emit thermal radiation, but always less than a blackbody at the same temperature. The treatment of non-blackbody radiation is usually based on a rigorous but somewhat abstract thermodynamic argument that tends to obscure the physical processes giving rise to the observed effects. We consider here an alternative somewhat simplistic but otherwise very helpful model, in which it is shown that an opaque isothermal material can be considered to be filled with blackbody radiation that is continually being absorbed and re-radiated. The outbound radiant flux that originates in a layer just beneath the surface is partially internally

reflected at the surface, in the case of optically homogeneous semi-transparent materials, or from scattering sites just beneath the surface, in the case of strongly scattering dielectrics. The fraction that penetrates the surface and is emitted is defined to be the spectral emissivity, $\varepsilon(\lambda)$, and the fraction that is internally reflected and re-absorbed can be recognized as the spectral reflectance, $\rho(\lambda)$.

As an example, we consider the combined effects of volume absorption and emission, together with surface reflection, on radiation from a thin elemental isothermal slab (Fig. 4) lying a short distance $x$ beneath and parallel to the surface of a thick optically homogeneous semi-transparent semi-infinite solid. For simplicity, we consider only radiation normal to the surface; this does not lead to an error. By Kirchhoff's law, we know that the spectral emissivity of the slab must be equal to its spectral absorptivity:

$$\varepsilon(\lambda) = \alpha(\lambda) = a(\lambda) \cdot dx \qquad (5)$$

where $a(\lambda)$ is the spectral linear absorption coefficient, the fraction of radiation absorbed per unit path length. The radiance emitted by the elemental slab $[a(\lambda) \cdot dx] \cdot L_{\lambda,b}(\lambda,T)$ in the direction of the surface and normal to it is reduced by absorption by a factor $e^{-a(\lambda) \cdot x}$ and is then

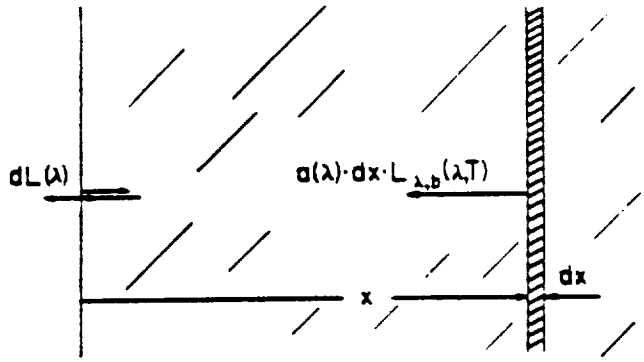


Fig. 4.

further reduced by surface reflection by a factor $1 - \rho(\lambda)$. Thus the contribution to the surface spectral radiance by the elemental slab is

$$dL(\lambda) = [1 - \rho(\lambda)] \cdot e^{-a(\lambda) \cdot x} \cdot [a(\lambda) \cdot dx] \cdot L_{\lambda,b}(\lambda,T) \qquad (6)$$

For a semi-infinite solid slab of thickness x great enough that radiation reflected from the back surface can be neglected,

$$L(\lambda) = [1 - \rho(\lambda)] \cdot L_{\lambda,b}(\lambda,T) \int_0^x e^{-a(\lambda) \cdot x} \cdot a(\lambda) \cdot dx \qquad (7)$$

Upon integration, this yields

$$L(\lambda) = [1 - \rho(\lambda)] \cdot [1 - e^{-a(\lambda) \cdot x}] \, L_{\lambda,b}(\lambda,T) \qquad (8)$$

From the formal definition of spectral emissivity,

$$L_\lambda(\lambda) \equiv \varepsilon(\lambda) \cdot L_{\lambda,b}(\lambda,T) \quad ; \qquad (9)$$

it follows that

$$\varepsilon(\lambda) = [1 - \rho(\lambda)] \cdot [1 - e^{-a(\lambda) \cdot x}] \qquad (10)$$

If the material is thick enough that $e^{-a(\lambda)\cdot x}$ is negligible compared to unity, the material is said to be opaque. Under these conditions,

$$\varepsilon(\lambda) = 1 - \rho(\lambda) \ . \qquad (11)$$

An opaque isothermal body is thus seen to behave as if it were filled with blackbody radiation, part of which is internally reflected by the surface and re-absorbed in the interior of the body; the remainder penetrates the surface and is emitted. It follows that the emissivity of an opaque isothermal body can be described in terms of its reflectivity.

The spectral absorption coefficient varies with wavelength, sometimes markedly; a material specimen such as glass may therefore be opaque at some wavelengths and transparent or semi-transparent at others, whereas metals of appreciable thickness tend to be opaque at all wavelengths. Eq.(10) applies in all cases, but only in spectral regions in which an isothermal body is opaque does it behave as if it were filled with blackbody radiation.

## SURFACE ROUGHNESS

The effects of surface roughness are difficult to predict quantitatively, largely because there is presently no fully satisfactory method of characterizing surface topography. Statistical descriptions have been used successfully in some applications. One of the more useful parameters is the optical roughness, $\sigma/\lambda$ , where $\sigma$ is the root mean square of the depth of the surface irregularities. When $\sigma/\lambda > 1$, the reflective behavior is determined by geometrical optics, but when $\sigma/\lambda << 1$, the reflective properties depend on diffraction. (DeWitt [2] gives $\sigma/\lambda = 0.15$ as the upper limit of the diffraction range.) Between these two regions, the reflective properties depend on the wavelength and the character of the surface topography [3] and are not well understood.

We know from Kirchhoff's law that, for any given direction from the surface and for any given component of polarization, the spectral absorptivity of a surface is equal to its spectral emissivity, i.e.,

$$\alpha(\lambda) = \varepsilon(\lambda) \quad . \tag{12}$$

This allows us to explain the fact that a roughened surface always has a higher emissivity than a smooth surface of

the same material (Fig. 5 and 6). If one considers radiation incident on a surface for which $\sigma/\lambda > 1$, where geometrical optics applies, a ray striking a smooth flat surface can reflect only once before leaving the surface, whereas a ray striking a pit may be reflected more than once before leaving the pit. The deeper the pit relative to its width, the greater the probable number of reflections that will occur before that radiant flux leaves the pit. Since some energy is absorbed at each reflection, a larger fraction of incident radiation is absorbed by a pit, on the average, than by a smooth surface. Since the absorptivity of the pitted surface is therefore higher than that of the smooth surface, so must be its emissivity, in accordance with Kirchhoff's law. The effects of surface roughness in the case of aluminum can be seen in Fig. 5 and 6.

For the case in which $\sigma/\lambda << 1$, diffraction dominates the directional distribution of reflected radiation. Assuming a Gaussian distribution of $\sigma$, Bennett and Porteus [7] extended earlier work done by Davies [8] and Chinmayanandam [9], based on diffraction theory, to obtain the following expression for the special case of normally incident irradiation:

$$\frac{\rho}{\rho_0} = e^{-(4\pi\cdot\sigma/\lambda)^2} + 32\cdot\pi^4\cdot(\sigma/\lambda)^4\cdot(\Delta\theta)^2/m^2 \qquad (13)$$

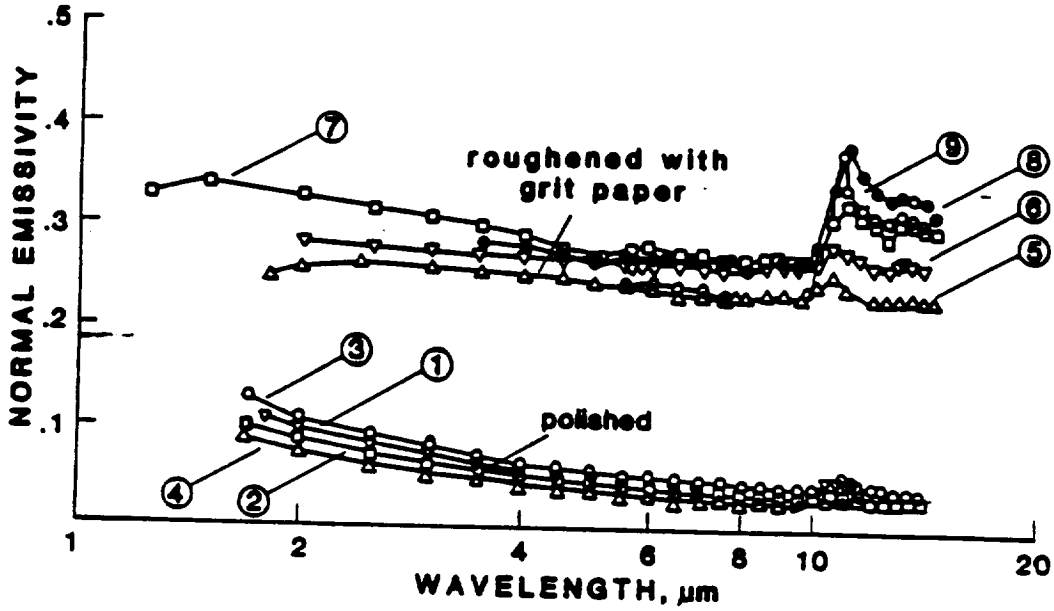


Fig. 5. Normal spectral emissivity of aluminum 11XX series. See Table 1 for experimental details.

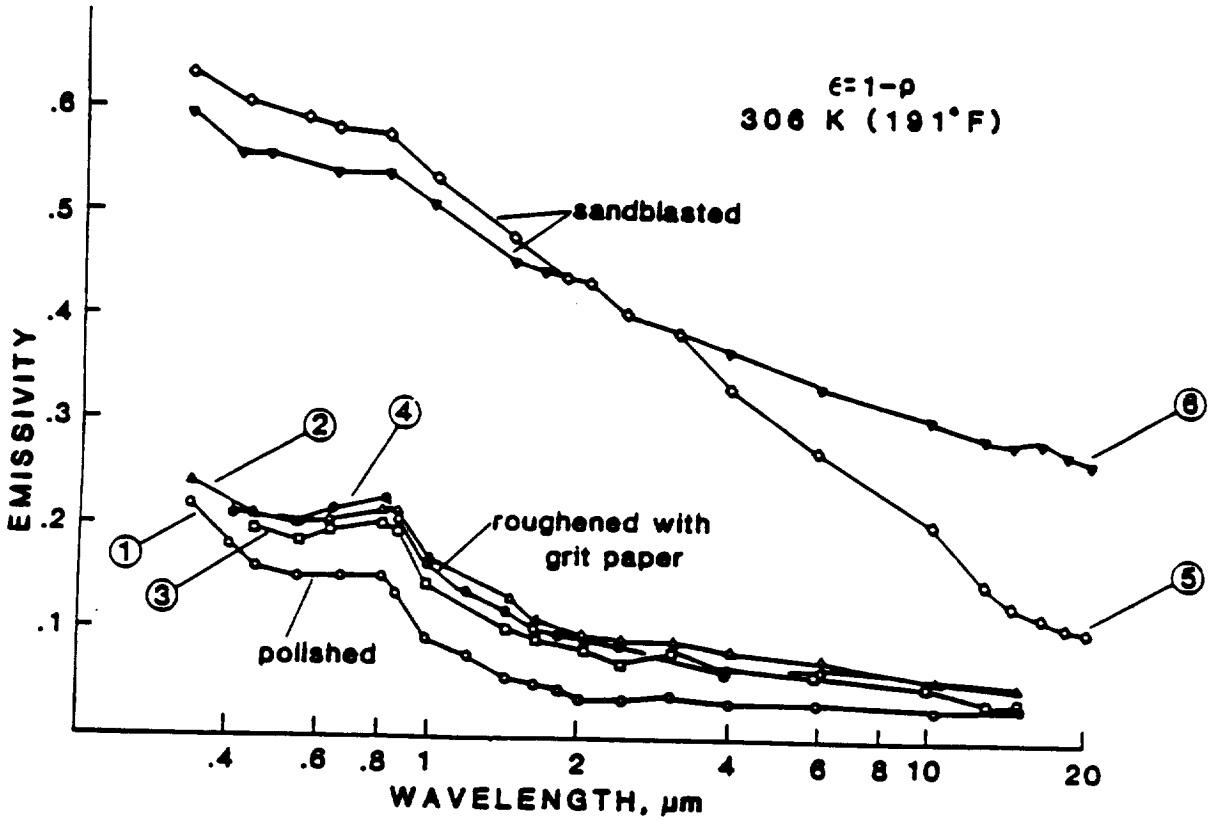


Fig. 6. Angular spectral emissivity of alloy 7075 (aluminum + Zn 7.5% + Mg 2.5% + Cu 1.6%) measured at 25° to the normal. See Table 2 for experimental details.

TABLE 1

Sample description and conditions for normal spectral emissivity of aluminum, 11XX series shown in Fig. 5 [4].

| Curve No. | Temperature K | Reported Error, % | Composition (Weight Percent), Specification and Remarks |
|---|---|---|---|
| 1 | 599 | ±20 | 99.7 Al, 0.11 Si, 0.01 Cu, 0.01 Mg, <0.01 Mn, Ni and Zn; cylindrical tube; heated at 467K for 15 hrs; polished with Carnu on Selvyt cloth; surface roughness 0.08 μm (center line average); data extracted from smooth curve; error given in the wavelength range 2 to 10 μm. |
| 2 | 697 | ±20 | Above specimen and conditions except heated at 697K for 20 hrs before measurement. |
| 3 | 805 | ±20 | Above specimen and conditions except heated at 805K for 15 hrs before measurement. |
| 4 | 599 | ±20 | Above specimen and conditions. |
| 5 | 462 | ±10 | 99.7 Al, 0.11 Fe, 0.11 Si, 0.01 Cu, 0.01 Mg, <0.01 Mn, Ni and Zn; tube; heated for 25 hrs at 462K; roughened and knurled with grade 180 silicon carbide paper, surface roughness 2.9 μm (center line average); data extracted from a smooth curve; error given over the wavelength range 2 to 10 μm. |
| 6 | 599 | ±10 | Above specimen and conditions except heated at 598K for 22 hrs before measurement. |
| 7 | 715 | ±10 | Above specimen and conditions except heated at 715K for 27 hrs before measurement. |
| 8 | 803 | ±10 | Above specimen and conditions except heated at 787K for 17 hrs before measurement. |
| 9 | 461 | ±10 | Above specimen and conditions. |

NOTE: Original publication is reference [5].

TABLE 2

Sample description and conditions for angular spectral emissivity of 7075-T6 alloy shown in Fig. 6 [4].

| Curve No. | Temperature K | Composition (Weight Percent), Specification and Remarks |
|---|---|---|
| 1 | 306 | Aluminum 7075-T6; nominal composition: 5.6 Zn, 2.5 Mg, 1.6 Cu, 0.30 Cr, and Al balance, polished surface roughness .08 μm (RMS); authors assumed $\varepsilon=\alpha=1-\rho$ (25°, 2π). |
| 2 | 306 | Aluminum 7075-T6; nominal composition: 5.6 Zn, 2.5 Mg, 1.6 Cu, 0.30 Cr, and Al balance; sanded with 150 grit paper (grit sieve opening 104 μm); RMS surface roughness in microinches; in line 0.3 μm, across 2 μm; authors assumed $\varepsilon=\alpha=1-\rho(25°,2\pi)$. |
| 3 | 306 | Aluminum 7075-T6; nominal composition: 5.6 An, 2.5 Mg, 1.6 Cu, 0.30 Cr and Al balance; sanded with 80 grit paper (grit sieve opening 175 μm); RMS surface roughness in microinches; in line 1 μm, across 4 μm; authors assumed $\varepsilon=\alpha=1-\rho(25°,2\pi)$. |
| 4 | 306 | Aluminum 7075-T6; nominal composition: 5.6 Zn, 2.5 Mg, 1.6 Cu, 0.30 Cr and Al balance; sanded with 40 grit paper (grit sieve opening 42 μm); RMS surface roughness in microinches; in line 1.9 μm, across 7.3 μm; authors assumed $\varepsilon=\alpha=1-\rho(25°,2\pi)$. |
| 5 | 306 | Aluminum 7075-T6; nominal composition: 5.6 Zn, 2.5 Mg, 1.6 Cu, 0.30 Cr and Al balance; sandblasted with 250 mesh silicon carbide (mesh opening 60 μm); RMS surface roughness .3 μm; authors assumed $\varepsilon=\alpha=1-\rho(25°,2\pi)$. |
| 6 | 306 | Aluminum 7075-T6; nominal composition: 5.6 Zn, 2.5 Mg, 1.6 Cu, 0.30 Cr and Al balance; sandblasted with 60 mesh silicon carbide (mesh opening 250 μm); RMS surface roughness 7 μm; authors assumed $\varepsilon=\alpha=1-\rho(25°, 2\pi)$. |

NOTE: Original publication is reference [6].

where $\rho$ is the reflectance of the roughened surface for normally incident radiation, $\rho_0$ is the corresponding reflectance of an ideally smooth surface, $\Delta\theta$ is the half angle of the field of view and $m$ is the rms slope of the pitted surface. This expression was experimentally verified for aluminized ground glass surfaces, with good accuracy. The first term on the right corresponds to specular (coherent) reflection and the second to diffuse reflection. Note that specular reflection dominates at long wavelengths and diffuse reflection dominates at short wavelengths. A more complete treatment of the scattering of electromagnetic waves from rough surfaces can be found in reference [10].

## OXIDATION

Oxidation can also have a major effect on the emissivity of metal surfaces [1]. We consider aluminum as an example. A tightly bound oxide barrier layer is formed on an initially unoxidized surface, impeding the rate of subsequent oxidation. A porous oxide layer then grows more gradually on top of the barrier layer. In the case of relatively pure aluminum (Fig. 7), these layers have only a small effect on the emissivity, but alloys containing magnesium are much more strongly affected. For all aluminum alloys containing significant amounts of magnesium, heating at a fixed temperature above 317 deg C (603 deg F) causes emissivity to

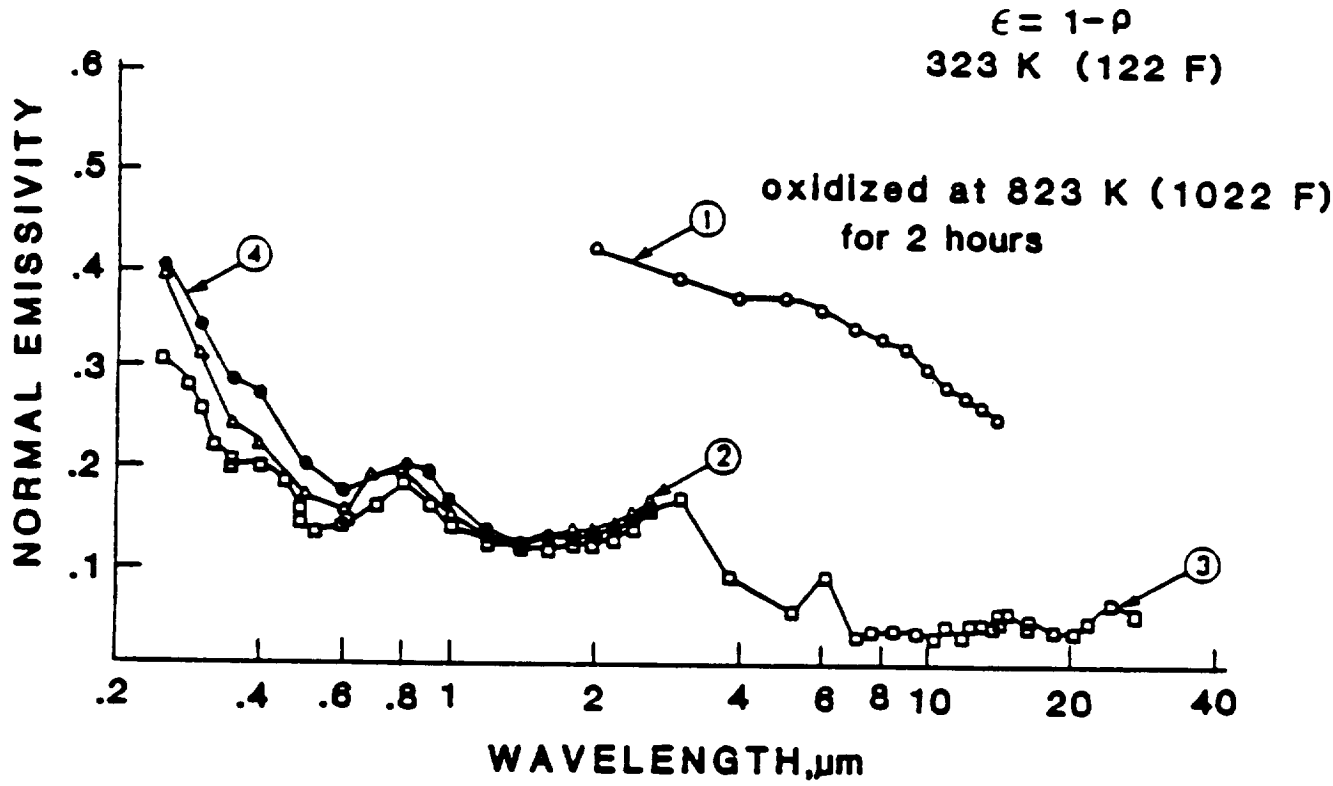


Fig. 7. Normal spectral emissivity of alloy 2024 (Aluminum + Cu 4.4% + Mg 1.5% + Mn 0.6%). See Table 3 for experimental details.

TABLE 3

Sample description and conditions for normal spectral emissivity of 2024 alloy shown in Fig. 7 [4].

| Curve No. | Temperature K | Composition (Weight Percent), Specifications and Remarks |
|---|---|---|
| 1 | 823 | Aluminum alloy 2024; nominal composition; 4.5 Cu, 1.5 Mg, 0.6 Mn, Al balance; oxidized in air for 2 hrs; measured in air. |
| 2 | 323 | Aluminum alloy 2024; nominal composition; 4.5 Cu, 1.5 Mg, 0.6 Mn, Al balance; surface roughness 0.04 μm (center line average); measured in nitrogen; computed by $\varepsilon=1-\rho(2\pi,5°)$, [Author's designation Specimen 1]. |
| 3 | 323 | Different sample, same as above specimen and conditions except surface roughness 0.2 μm (center line average); [Author's designation: Specimen 3]. |
| 4 | 323 | Different angle, same as above specimen and conditions except surface roughness 0.08 μm (center line average); [Author's designation: Specimen 4]. |

NOTE: Original publication is reference [4] for curve 1 and reference [12] for curves 2, 3 and 4.

increase at a rate that is a function of the magnesium concentration, nearly independently of other factors. This effect has its roots in the relatively high vapor pressure of magnesium, which causes the magnesium to migrate to the surface where it either evaporates or oxidizes. This causes roughening of the interface between the alloy and the oxide, thus increasing the emissivity. The outward migration of magnesium also causes dislodged microscopic aluminum be trapped in the oxide layer, further increasing the emissivity due to optical scattering effects. The effects of oxidation are illustrated in Fig. 7. Haugh [1] found oxidation to be "the most serious obstacle for applying radiation thermometry to aluminum alloys." This problem could be largely eliminated if a satisfactory method could be found for measuring the emissivity of aluminum alloys during the manufacturing process.

Emissivity effects for opaque surfaces can thus be accounted for in terms of reflection effects, and a knowledge of the reflective properties of such a surface forms much of the basis for an understanding of its emissivity. For a closer look at reflectance effects, we now consider some well-known conclusions from electromagnetic field theory.

## FRESNEL REFLECTION

The Fresnel formulas, which can be derived from Maxwell's equations, are expressions for the reflectivity of an ideally smooth (specular) and optically homogeneous plane material surface for incident electromagnetic radiation. The polarized components of reflectivity are expressed in terms of the optical "constants" n (the refractive index) and $\kappa$ (the extinction coefficient) of the surface material, and $\theta$, the angles of incidence and reflection. These are given below for two orthogonal components of polarization:

$$\rho_{\lambda\parallel}(\lambda,\theta) = \frac{a^2 + b^2 - 2\cdot a\cdot\sin\theta\cdot\tan\theta + \sin^2\theta\cdot\tan^2\theta}{a^2 + b^2 + 2\cdot a\cdot\sin\theta\cdot\tan\theta + \sin^2\theta\cdot\tan^2\theta}\,\rho_{\lambda\perp}(\lambda,\theta) \qquad (14)$$

$$\rho_{\lambda\perp}(\lambda,\theta) = \frac{a^2 + b^2 - 2\cdot a\cdot\cos\theta + \cos^2\theta}{a^2 + b^2 + 2\cdot a\cdot\cos\theta + \cos^2\theta} \qquad (15)$$

where

$$2\cdot a^2 = [(n^2 - \kappa^2 - \sin^2\theta)^2 + 4\cdot n^2\cdot\kappa^2]^{1/2} + n^2 - \kappa^2 - \sin^2\theta \qquad (16)$$

and

$$2\cdot b^2 = [(n^2 - \kappa^2 - \sin^2\theta)^2 + 4\cdot n^2\cdot\kappa^2]^{1/2} - (n^2 - \kappa^2 - \sin^2\theta) \qquad (17)$$

where $\rho_{\perp}$ is the reflectivity for plane polarized incident radiation with the direction of vibration of the electric vector perpendicular to the plane of incidence and $\rho_{\parallel}$ is the reflectivity when the direction of vibration of the electric vector is parallel to the plane of incidence. Note that the refractive index $n$ and extinction coefficient $\kappa$ properties of the material, are both dependent on wavelength and, at least to some extent, on temperature, and are therefore not truly constants.

Since an incident plane polarized wave of any orientation can always be resolved into two orthogonal components, one perpendicular and one parallel to the plane of incidence, the above expressions are sufficient to cover all cases of specular reflectance.

It can be shown that eq.(11) holds for each of the polarized components:

$$\varepsilon_{\perp}(\lambda) + \rho_{\perp}(\lambda) = 1 \qquad (18)$$

and

$$\varepsilon_{\parallel}(\lambda) + \rho_{\parallel}(\lambda) = 1 \qquad (19)$$

and that for unpolarized incident radiation,

$$\rho(\lambda) = \frac{1}{2} \cdot [\rho_{\perp}(\lambda) + \rho_{\parallel}(\lambda)] \qquad (20)$$

Plots of the reflectivities corresponding to eq.(14), (15), and (20) are given in Fig. 8 for a range of values of $n$ and $\kappa$, and for angles of incidence up to 90 degrees. The extinction coefficient, and therefore the reflectivity, is characteristically low in materials classified as dielectrics, is characteristically high in materials classified as electrical conductors, and is very high in the case of resonance absorption. For dielectrics, typically $1.3 < n < 3$, and $\kappa < 1$. Values of $n$ and $\kappa$ for a number of metals are given in Table 4, for a few selected wavelengths.

Changes in the phase angle of an incident wave occur during the reflection process, giving rise to additional polarization effects. As a result, thermal radiation from a smooth metallic surface viewed off-normal is elliptically polarized. In the case of a rough surface, on the other hand, the angle of incidence of a beam of radiation depends on the surface micro-topography and varies across the width of the beam. The reflected radiation thus contains many different components of polarization, the net effect of which is difficult to characterize in practice. An understanding of these and other such effects is likely to be important to future

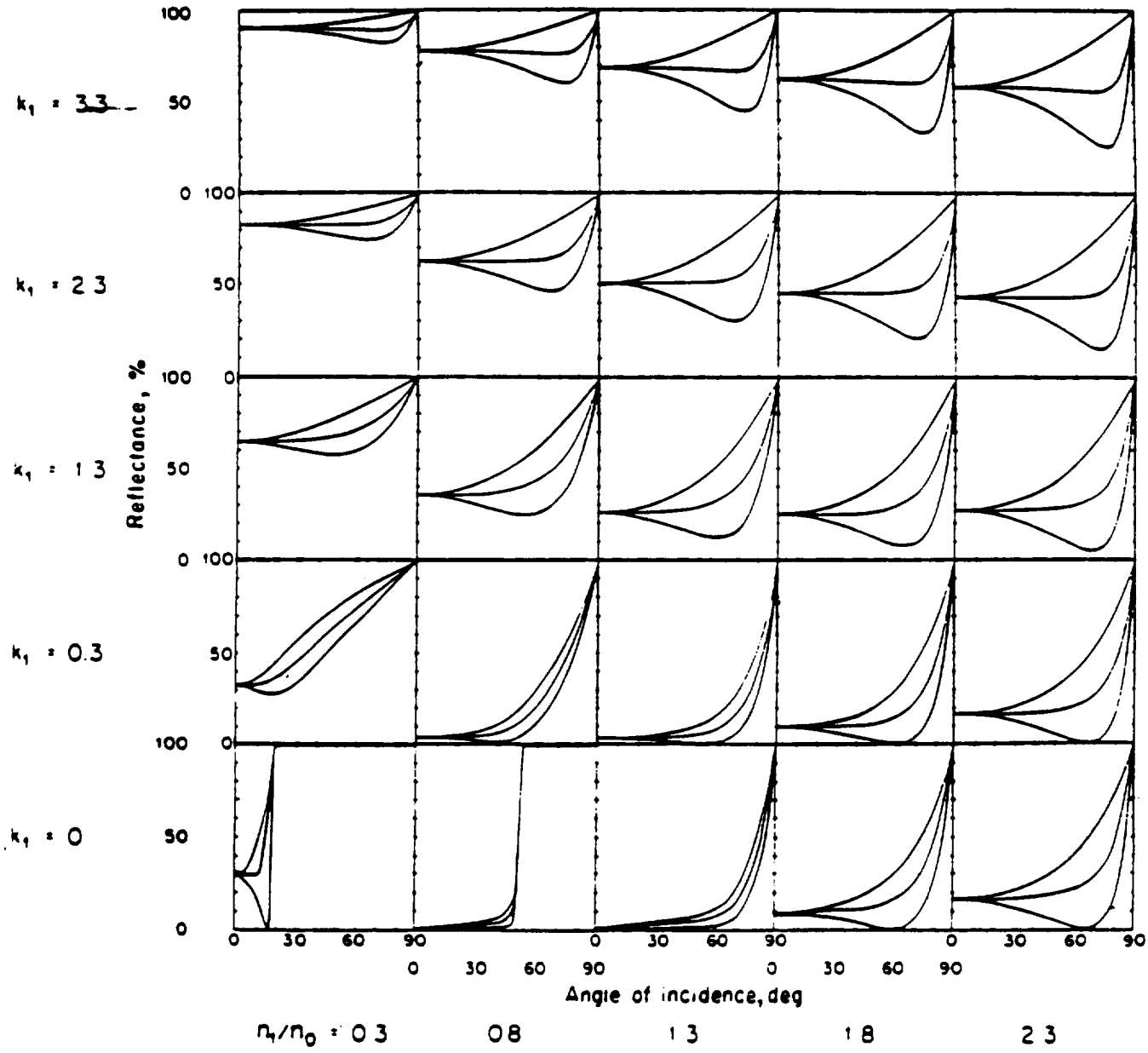


Fig. 8. $\rho_{\perp}$ (upper curves), $\rho_{\parallel}$ (lower curves), and $\rho_{av} = (\rho_{\perp} + \rho_{\parallel})/2$ as a function of angle of incidence for various values of the refractive index ratio $n_1/n_0$ and $\kappa_1$. The incident medium, having refractive index $n$, is assumed to be non-absorbing. Adapted from J.M. & H.E. Bennett, Handbook of Optics [13].

TABLE 4

Optical Constants of Selected Metals

| | λ | n | κ |
|---|---|---|---|
| Aluminum | 12 μm | 33.6 | 76.4 |
| Cobalt | 0.589 | 2.120 | 1.900 |
| Copper | 0.650 | 0.44 | 3.26 |
| | 2.25 | 1.03 | 11.7 |
| | 4.00 | 1.87 | 21.3 |
| | 4.20 | 1.92 | 22.8 |
| | 5.50 | 3.16 | 28.4 |
| Gold | 0.589 | 0.47 | 2.83 |
| | 2.00 | 0.47 | 12.5 |
| | 5.00 | 1.81 | 32.8 |
| Iron | 0.589 | 1.51 | 1.63 |
| Magnesium | 0.589 | 0.37 | 4.42 |
| Nickel | 0.589 | 1.79 | 3.33 |
| | 2.25 | 3.95 | 9.20 |
| Platinum | 5.00 | 11.5 | 15.7 |
| Silver | 0.589 | 0.18 | 3.64 |
| | 2.25 | 0.77 | 15.4 |
| | 4.37 | 4.34 | 32.6 |
| | 4.50 | 4.49 | 33.3 |
| Sodium | 0.589 | 0.005 | 522 |
| Steel | 0.589 | 2.485 | 1.381 |

NOTE: There are often significant differences between values for optical constants determined by different investigators. Those given above are typical.

developments in radiation thermometry, since consideration of the polarized components of radiation taken separately offers significant potential advantages over the consideration only of unpolarized radiation. As an example, consider the reflectivities illustrated in Fig. 8 It is clear that $\rho_{\parallel}$ is much smaller than $\rho_{\perp}$ in certain angular regions off-normal, and therefore that $\varepsilon_{\parallel}$ is much larger than $\varepsilon_{\perp}$ at those angles. Similarly, $\varepsilon_{\parallel}$ is substantially larger than the unpolarized emissivity in those regions. The existence of polarized components of reflectivity and emissivity also creates the possibility of other useful relationships, such as Abele's condition [14]. For a further discussion of polarization effects, the reader is referred to standard texts on optics [15,16].

The Fresnel formulas are reliable to the extent that surface conditions approach the ideal and the correct values of the optical constants are known. In practice, surface conditions are often far from ideal and optical constants can be strongly affected by the presence of impurities and inhomogeneities. When allowances are made for non-ideal surface conditions such as roughness, impurities, inhomogeneities and coatings, however, the Fresnel formulas provide a sound basis for understanding emissivity effects.

The values of the optical constants can be determined experimentally by a sophisticated experimental procedure known as ellipsometry [13]. This requires very nearly ideal optically smooth homogeneous surfaces of the material under consideration. In the case of pure aluminum, such surfaces can be prepared by vacuum vapor-deposition on an optically flat glass plate. When values of $n$ and $\kappa$ determined by ellipsometry for vapor deposited aluminum are substituted into the Fresnel equations, the computed values of spectral reflectance compare very favorably with experimentally determined values [1], as can be seen in Fig. 9.

Expressions for $n$ and $\kappa$ can also be deduced from quantum theory and expressed in terms of atomic constants and wavelength, so it is possible in principle to determine emissivity from physical theory. Since the appropriate physical constants are not all sufficiently well known in practical situations, however, emissivities are determined experimentally in practice. The theory is used primarily to correlate emissivity values obtained experimentally under one set of conditions with the corresponding values to be expected under a different set of conditions, most commonly at different temperatures.

Free electron theory, which allows predictions of emissivity as a function of electrical resistivity and wavelength, is

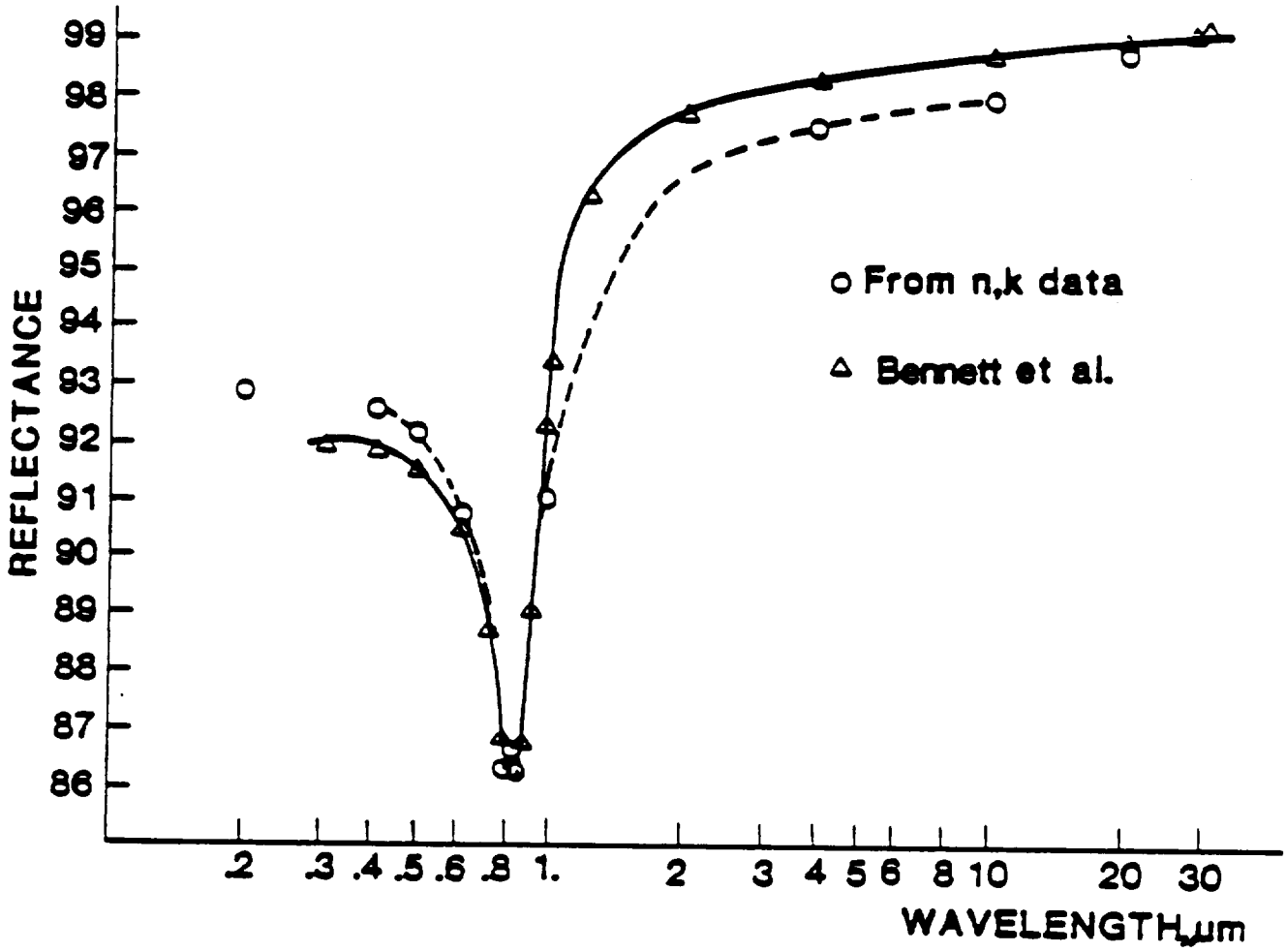


Fig. 9. Experimental values for spectral reflectivity of aluminum vacuum evaporated on optical plate. See Table 5 for numerical values.

TABLE 5

Experimentally Determined Reflectance for
Aluminum Vacuum Evaporated on Optical Plate

| λ mu | 1 | 2 | 3 |
|---|---|---|---|
| | Reflectance | | |
| .2 | .928 | | |
| .4 | .926 | | .919 |
| .65 | .907 | | .906 |
| .8 | .864 | | .868 |
| .95 | .912 | | .924 |
| 1.0 | | | .940 |
| 1.2 | | | .964 |
| 1.5 | | | .974 |
| 2. | .968 | | .978 |
| 4. | .975 | | .983 |
| 6. | .978 | | .986 |
| 8. | .979 | | .987 |
| 10. | .980 | .978 | .988 |
| 12. | .982 | | .988 |
| 14. | | .984 | |
| 16. | | .988 | .989 |
| 18. | | .989 | .990 |
| 20. | | .989 | .990 |
| 22. | | | .991 |
| 24. | | | .991 |
| 26. | | | .992 |
| 28. | | | .992 |
| 30. | | | .993 |

1. Hess[17], Schultz [18]; from n and K values.
2. Lenhan [21]; from n and K values.
3. Bennett [22]; direct measurement.

accurate only at wavelengths longer than those ordinarily used for radiation thermometry. Discussions of free electron theory as it applies to predicting emissivity can be found in reference [4], with examples in the case of aluminum in reference [1].

## SUBSURFACE EFFECTS IN DIELECTRICS

The depth to which radiation penetrates is much greater in dielectrics than in electrical conductors, and the reflectivity of the air-dielectric interface is much lower. Emission from dielectrics, being primarily a volume effect, therefore tends to be diffuse. Since reflection by the air-dielectric interface is a relatively small effect, surface roughness plays only a minor role.

The decrease in emissivity for angles approaching the tangent of optically smooth and homogeneous materials is caused by refraction and internal reflection of internally emitted radiation. In the case of dielectrics (Fig. 10), total internal reflection occurs for off-normal angles beyond the critical angle, which is determined by the refractive index. This is not true of conductors, which tend to have their maximum emissivity at around 75-85 degrees off normal (for ideally smooth surfaces), with the emissivity dropping to zero along the tangent as in the case

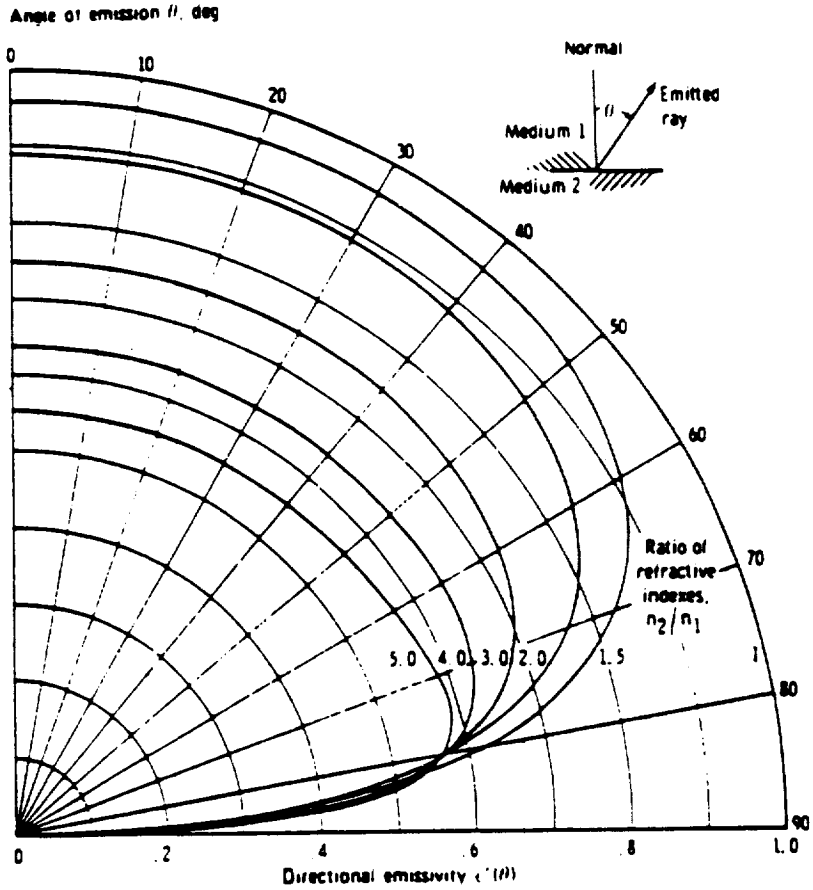


Fig. 10. Directional emissivity of an optically smooth opaque dielectric, as predicted from electromagnetic theory [23], for unpolarized radiation.

of dielectrics. The maximum in the emissivity of conductors is caused by the minimum in the reflectivity at those angles, as seen in Fig. 8. The tendency for diffuse emission by dielectrics is further enhanced when the material is optically inhomogeneous, as in the case of polycrystalline dielectrics, where reflection by subsurface scattering from grain boundaries, pores and inclusions dominates both the reflectance and the emissivity. Thus we see that there is a characteristic difference between the emissivity of dielectrics (high and diffuse) and that of metals (low and substantially more directional).

## COMPLEMENTARITY

Eq.(11) provides us with an indirect but commonly used way to determine the spectral emissivity of opaque surfaces, that is, by measuring spectral reflectance. Care must be taken, however, to assure that the kind of spectral reflectance measured is complementary to the kind of spectral emissivity desired. In radiation thermometry, one ordinarily wants directional rather than hemispheric spectral emissivity, and the complementary quantity is the directionally incident-hemispherically reflected spectral reflectance. This can be seen by considering a ray incident on a surface, which may be either diffuse or specular, from direction i. A fraction $\alpha_i(\lambda)$, the spectral directional absorptivity, is

absorbed and the remaining fraction $\rho_{ih}(\lambda)$, the spectral directional-hemispherical reflectance, is reflected into the hemisphere above the surface. From the conservation of energy, we therefore have

$$\alpha_i(\lambda) + \rho_{ih}(\lambda) = 1 \quad . \tag{21}$$

It follows directly from Kirchhoff's law that

$$\varepsilon_i(\lambda) + \rho_{ih}(\lambda) = 1 \tag{22}$$

This implies that the reflectance must be that corresponding to directionally incident radiation reflected into the hemisphere above the surface, where the direction of incidence is the opposite of that in which the emissivity is desired. From the Helmholtz reciprocity theorem [24], it is known that the reflectance for hemispherically incident-directionally reflected radiation is the same as that for directionally incident-hemispherically reflected radiation. Helmholtz reciprocity applies in the vast majority of cases encountered in radiation thermometry. Measurements are usually made with hemispherically-incident radiation, for which appropriate measurement techniques have been developed [25]. Note also that if such measurements are made at one temperature, such as room temperature, the actual values of spectral reflectance and spectral emissivity will be somewhat

different at other temperatures because of at least some degree of temperature dependence in the optical constants.

## ENVIRONMENTAL EFFECTS

### ATMOSPHERIC EFFECTS

The optical medium between the thermally radiating target and the radiation thermometer includes atmospheric gases, vapors, dust and any windows that might be in the sight path. The atmosphere in most cases is composed of gaseous nitrogen, oxygen, water and carbon dioxide, with other gases also present to a significant extent in a variety of industrial processes. These gases, vapors and dust particles absorb, emit and scatter radiation, and their effects on radiometric measurements range from negligible to severe. By Kirchhoff's law, emission is proportional to absorption. If the concentration and temperature of a vapor-free atmosphere were uniform, it would radiate in accordance with eq.(8), with $\rho(\lambda) = 0$; in practice, however, the concentration and temperature of these atmospheric constituents tend to be highly variable with time and position, and vapors are frequently present.

Although the physics of the absorption, emission and scattering processes is generally understood, the conditions under which it applies are highly variable and seldom well enough known quantitatively to allow for practical corrections to be determined and applied. Once recognized, however, this need not be a serious problem in most cases (gaseous absorption and emission), since there are spectral regions - known as atmospheric windows - in which the atmosphere does not absorb and therefore does not emit radiation. These spectral regions are clearly evident in Fig. 11. If radiometric measurements are confined to those spectral regions, atmospheric interference - in the absence of particulate scattering - is entirely negligible. When scattering effects are strong, however, as in the case of suspended particulates (dust), steam clouds or sooty flames, the use of an atmospheric window alone does not correct the problem. It is then common practice for the radiometer to view through a tube purged with a clean dry (transparent) gas, using a filter to limit the radiometer passband to an atmospheric window.

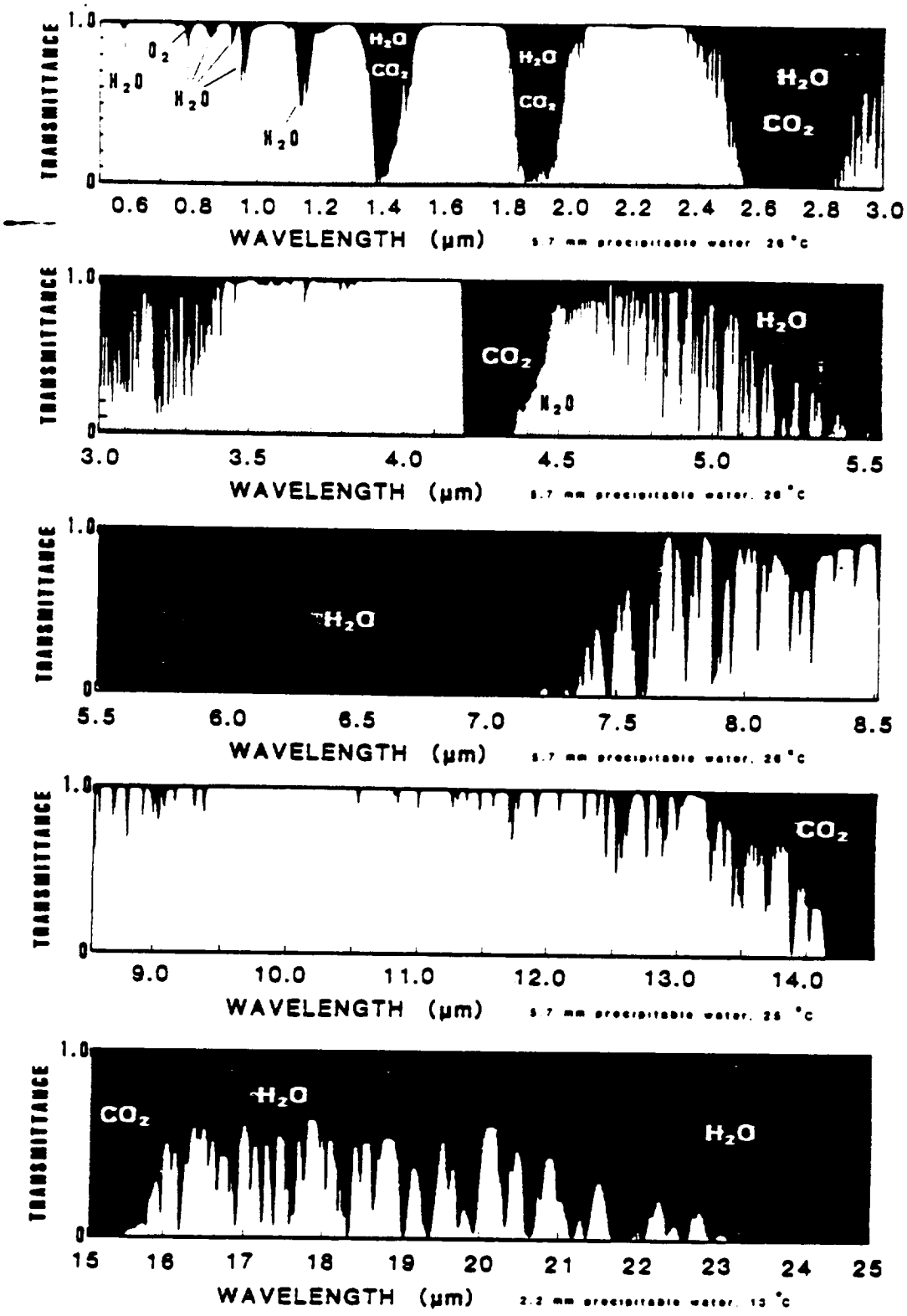


Fig. 11. Atmospheric transmission at sea level over a 300 meter path. From NRL report 5453 by H. W. Yates and J. H. Taylor, 1960 [26]. Adapted by G. D. Nutter

## REFLECTED RADIATION

Radiation originating from extraneous sources and reflecting from a target surface increases its spectral radiance and causes errors in radiometric temperature measurements:

$$L_\lambda(\lambda)_{observed} = L_\lambda(\lambda)_{emitted} + L_\lambda(\lambda)_{reflected} \qquad (23)$$

The magnitude of the reflected spectral radiance depends on the spectral radiance of the extraneous source, the solid angle subtended by it from the target area, and the bidirectional spectral reflectance distribution function of the target. When the magnitude of the reflected radiance is comparable to or larger than that of the emitted radiance, errors in temperature measurement tend to be large. This is most likely to occur when target temperatures are not greatly different from ambient temperature, and the problem intensifies as target temperatures decrease. At target temperatures below about 100-150 deg C, reflected radiation is usually the dominant source of error in radiation thermometry.

The target can often be successfully shielded from the extraneous radiation by a suitably placed screen. It is also sometimes possible to measure the reflected component separately with the aid of a relatively cool auxiliary reflector of known reflectance located near the target and

subjected to the same irradiance, and to then subtract that component from the observed spectral radiance (eq.(23)). The trend in recent years has been toward trying to develop techniques for dealing with reflected radiation, some of which have met with a significant degree of success [27].

## SEVERE AMBIENT TEMPERATURE AND DUST ENVIRONMENTS

It is frequently necessary to use radiation thermometers in severe environments such as those commonly found in industry, where the high temperatures would destroy an unprotected instrument. Cooling is satisfactorily accomplished by the use of air or water flowing through tubes provided in the instrument housing to regulate its temperature. Air or some other dry gas to purge dust from the sight path and lens is also usually supplied through tubes in the instrument housing.

## WINDOWS

Radiation thermometers must often view targets through windows, thus reducing the spectral radiance by a factor equal to the (external) spectral transmittance $\tau(\lambda)$ of the window:

$$\frac{L_\lambda(\lambda,T)_{apparent}}{L_\lambda(\lambda,T)} = \tau(\lambda) \qquad (24)$$

A simple expression for the difference between the (true) temperature and the apparent temperature of the target viewed through the window can be obtained by substituting the expression for $L_{\lambda,b}(\lambda,T)$ from Wien's law into eq.(24):

$$\frac{1}{T} = \frac{1}{T_{apparent}} + \frac{\lambda}{c_2} \cdot \ln \tau(\lambda) \quad , \qquad (25)$$

where $\tau$ can be either the <u>mean effective wavelength</u> of the instrument or, if the spectral bandwidth is sufficiently narrow, the <u>reference wavelength</u>, which can be determined more accurately. The theory of effective and reference wavelengths is very important in high accuracy applications, such as in realizing the temperature scale, and has been highly developed [28,29,30]. The mean effective wavelength is an appropriately averaged wavelength that accounts for the spectral response characteristics of the radiometer and is found to be a function of $T$ and $T_{apparent}$ The reference wavelength, on the other hand, is determined primarily by the filter characteristics and is independent of $T$ and $T_{apparent}$.

For sufficiently narrow bandwidths, $\lambda$ is only very weakly dependent on $T$ and $T_{apparent}$, and we then define the "A-value" of the window such that

$$\frac{1}{T_{apparent}} - \frac{1}{T} \equiv A \quad . \tag{26}$$

In ordinary applications the A-value of the window is treated as a constant; once determined for any pair of temperatures, it can be used to relate any other pair of temperatures. The International Practical Temperature Scale above the gold point is generated in this manner from a single known temperature (a blackbody at the freezing temperature of gold, 1Ø64.43 deg C) using a set of filters of known transmittance and a known spectral band, except that the Planck distribution is used instead of Wien's law in eq.(24). This technique can also be used to extrapolate from any given temperature on one range of a radiation thermometer to a temperature on a higher range by viewing a target through a gray filter having a known A-value, thus calibrating the upper range in terms of the lower range as in the case of the disappearing-filament optical pyrometer.

# THE RADIATION THERMOMETER

## THE RADIOMETER MEASUREMENT EQUATION

The elemental radiant flux input to the radiometer (Fig. 1) from the target area $A_t$ into the solid angle $\omega_t$ is obtained from eq.(4):

$$\partial^3\Phi = L_\lambda(\lambda)\cdot\partial A_t\cdot\cos\theta\cdot\partial\omega_t\cdot\partial\lambda \qquad (27)$$

The radiant flux is attenuated by $\tau(\lambda)$, the spectral transmittance of the optical system, as determined primarily by a bandpass filter, and is then incident on the photodetector having a spectral responsivity $\mathcal{R}(\lambda)$; the photodetector generates an elemental output signal

$$\partial^3 S = \mathcal{R}(\lambda)\cdot\tau(\lambda)\cdot\partial^3\Phi = \mathcal{R}(\lambda)\cdot\tau(\lambda)\cdot L_\lambda(\lambda)\cdot\partial A_t\cdot\cos\theta\cdot\partial\omega_t\cdot\partial\lambda \qquad (28)$$

from which we have the radiometer measurement equation:

$$S = \int_\lambda\int_\omega\int_{A_t} \mathcal{R}(\lambda)\cdot\tau(\lambda)\cdot L_\lambda(\lambda)\cdot\partial A_t\cdot\cos\theta\cdot\partial\omega_t\partial\lambda \qquad (29)$$

From the Lagrange Invariant, $A_t \cdot \cos\theta\omega_t = A_{n,d} \cdot \omega_d$ , where $A_{n,d}$ is the projection of the field-defining aperture area normal to the optical axis and $\omega_d$ is the solid angle of radiant flux incident on that aperture. Where $L_\lambda(\lambda)$ varies only slowly with direction, we therefore have

$$S = A_{n,d} \cdot \omega_d \cdot \int_0^\infty \mathcal{R}(\lambda) \cdot \tau(\lambda) \cdot L_\lambda(\lambda) \cdot d\lambda \qquad (30)$$

If the spectral band $\delta\lambda$ centered about $\lambda$ is sufficiently narrow, the radiometer measurement equation can be simplified to the form

$$S = K(\lambda_c) \cdot L_\lambda(\lambda_c) \qquad (31)$$

where

$$K(\lambda_c) = A_{n,d} \cdot \omega_d \cdot \mathcal{R}(\lambda_c) \cdot \tau(\lambda_c) \cdot \delta\lambda \qquad (32)$$

Thus we see that the output signal of an ideal radiometer is directly proportional to the spectral radiance of the target.

---

The three dimensional form of the Lagrange Invariant is also known as the throughput, the geometric extent, or as the etendue of the beam.

This simplified form of the radiometer measurement equation, when used with an appropriately defined correction factor, can be used for high accuracy radiation thermometry with relative spectral bandwidths ( $\delta\lambda/\lambda$ ) up to about 10 %, using the reference wavelength [29]. For larger relative bandwidths, it is customary to use the mean effective wavelength [30]. For less accurate work, eq.(31) is commonly used - without the correction factor - because of its simplicity. For wide spectral bands, eq.(30) must be used.

## THE OPTICAL SYSTEM

The optical systems of most radiation thermometers used in industry are similar to that illustrated in Fig. 1, although many instruments also include a visual viewing system for alignment purposes. More sophisticated research laboratory instruments often have additional optical elements behind the field-defining aperture.

Some instruments use a mirror objective in place of the objective lens, ordinarily for the purpose of viewing low temperature targets where a very wide spectral band is required. Mirror objectives have the advantage of being fully achromatic, i.e., their focal length is independent of

wavelength. While reflective (mirror) and refractive (lens) objectives each have their advantages and disadvantages, single-element lenses are more widely used than mirror objectives in industrial radiation thermometers except for low temperature measurements.

Materials suitable for use in infrared optics are relatively few in number, and are much more costly than those used in the visible spectrum. Finding a material with the desired combination of properties is often difficult and sometimes impossible. The spectral transmittance of several of the most commonly used infrared optical materials are shown in Fig. 12. The spectral range of greatest interest in industrial applications is from about 1.5 to about 4 μm, with some applications out to 14 μm. The visible spectrum is from 400 to 780 nm (0.4-0.8 μm).

There are several other properties of optical materials that must also be taken into account. Many infrared optical materials tend to be hygroscopic, sharply limiting their usefulness in industrial radiation thermometers; those shown in Fig. 12 are non-hygroscopic.

The refractive index of any optical material varies systematically with wavelength. Since the focal length of the lens is a function of the refractive index, the focal length also

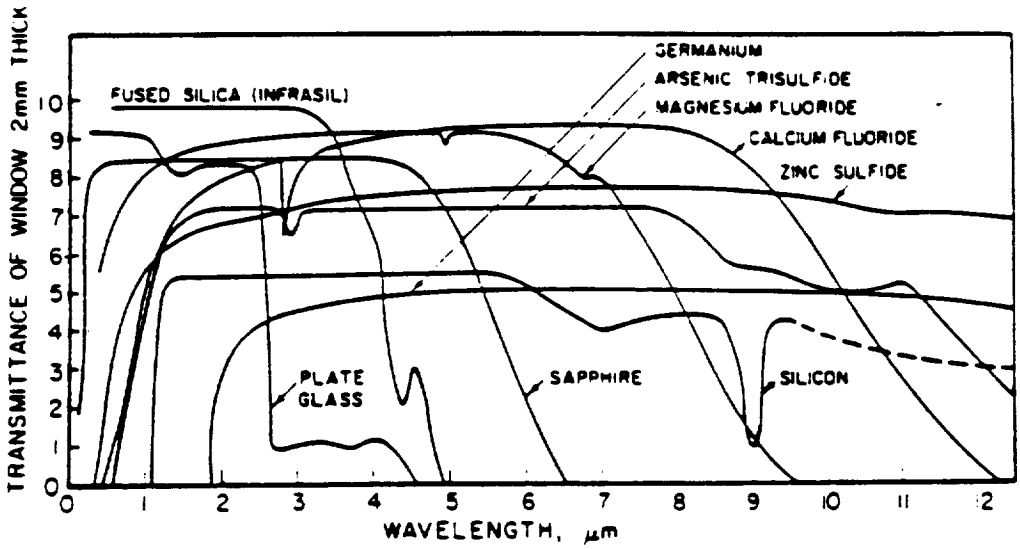


Fig. 12. Commonly used infrared optical materials.

diffraction limited even as a single element lens; however, it is opaque in the visible spectrum. Those, such as zinc sulfide, that have a high refractive index, transmit in the visible spectrum, and have other desirable properties, are very limited in number, and are expensive. Lenses having a low refractive index, such as fused silica and calcium fluoride, have a large amount of spheric aberration, making them unable to focus sharply on small targets and causing the target area to be larger than expected because of the blurred image.

## PHOTODETECTION

Photodetectors (Fig. 13) are classed as quantum detectors if they convert photons to charge carriers, or thermal detectors if they sense the heating effect of absorbed radiation. Both types are used in radiation thermometry Linearity of photodetector response is particularly useful in radiometry. as is stability of responsivity with time and temperature. A large variety of photodetectors is now commercially available. Those most widely used in radiation thermometry at present include PbS, PbSe, Si, InAr, InSb, thermopiles and pyroelectrics. Some of these exhibit linear response to radiant power input over dynamic ranges up to about nine orders of magnitude; others are linear only over much smaller ranges.

varies with wavelength (longitudinal chromatic aberration). An optical system with a simple objective lens designed to work at one wavelength is therefore likely to be unsuitable for simultaneous use at a substantially different wavelength, since it focuses at a different target distance for one wavelength than for the other. This can be a serious problem in instruments intended for spectral radiance measurements at more than one wavelength, particularly when the target is small. This also limits the extent to which an objective lens that is intended to transmit radiant power to the photodetector can also be used for visually aiming the instrument. The problem can sometimes be largely eliminated by achromatizing the lens. This is seldom done in industrial instruments, however, since it greatly increases the cost of an already expensive infrared lens, and often does not produce an otherwise high quality image except on or very near the optical axis. Mirror objectives are often used to eliminate chromatic aberration, since they are fully achromatic.

Spheric aberration is the only other significant lens aberration affecting the performance of "spot-type" radiation thermometers, and it can be controlled or eliminated by choosing a lens material that has a sufficiently large refractive index. There are several materials that work well for this purpose. The best is germanium, which can be

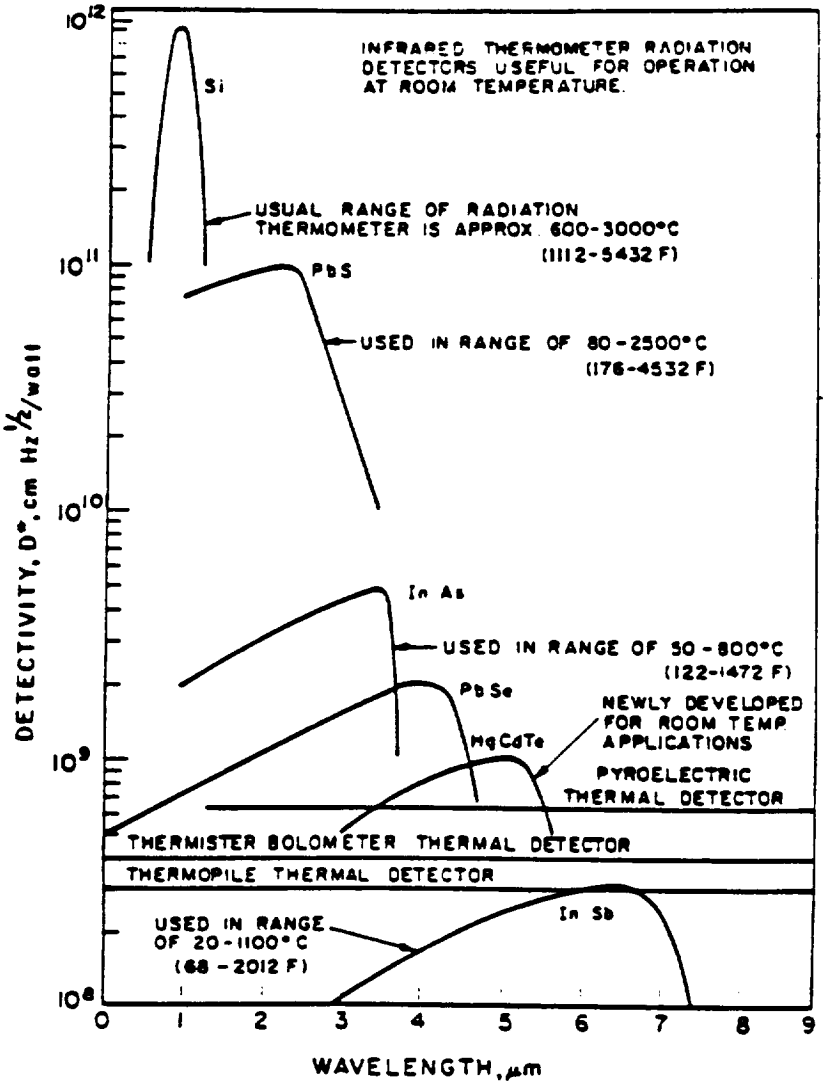


Fig. 13. Photodetectors commonly used in radiation thermometry, for room temperature operation.

The spectral responsivity of most quantum photodetectors is strongly temperature-dependent, requiring extensive use of temperature compensation techniques. Silicon photodiodes, used for the target temperature range above about 500 deg C, are especially noteworthy in that they have a highly linear response (over eight decades in many cases), their responsivity is nearly independent of temperature over a significantly wide spectral range, and special techniques have recently been developed for their accurate "self-calibration" [31].

Those detectors that perform best in the spectral range best suited to radiation thermometry in the metals industries (about 1.5 to 2.5 $\mu$m) tend to need a substantial amount of ambient temperature compensation. The responsivity of lead sulfide, for example, changes by about 3% per degree C change in ambient temperature. This is an area in which present day industrial radiation thermometers are in need of improvement if they are to meet the tightest tolerances required by industry. Suitable technology presently exists to do this, primarily through the use of temperature-regulated thermoelectric coolers to cool and regulate the temperature of the photodetectors. Some industrial radiation thermometers already use thermoelectric cooling, but most are not sufficiently well temperature regulated, holding the detector temperature constant only to within about 1 degree

C. The principal disadvantage to this approach is the increased cost of the instrumentation.

Radiation thermometry is frequently concerned with very low-level signals, where noise is a significant factor. Noise is present in the photon stream due to the statistics of photon emission. Noise also originates in the detector itself, where it is described in terms of the specific spectral detectivity, $D^*(\lambda)$, of the detector, and finally, noise is introduced in the amplification process. The use of modulated - or "chopped" - radiation permits the use of ac amplification; this introduces less noise than dc amplification and serves to eliminate much of the signal component due to unwanted "background" radiation. The effects of noise are controlled by filtering, in combination with the selection of various optical system parameters in the measurement equation. Noise ultimately sets the limit to temperature resolution in radiation thermometry.

Long-term changes in the spectral responsivity of photodetectors or their temperature compensation are often accommodated by the use of some form of internal reference standard such as an incandescent or solid state lamp. The internal reference standard in such cases has been determined to be much more repeatable over an extended period of time than is the responsivity of the photodetector. In some instruments

using highly sensitive but unstable detectors (e.g., PbS), the reference source is used continuously in a radiation null-balancing system. The disappearing-filament optical pyrometer is an early example of such a system; automated versions of that and other null-balancing instruments now exist.

## HIGH POWER OF T

Much of the behavior characteristic of narrow-band radiation thermometers can be understood by expressing thermally emitted spectral radiance in terms of a power of the temperature , i.e.,

$$L \alpha T^n \tag{33}$$

Where Wien's law is a suitable approximation, it can be shown that

$$n = \frac{c_2}{\lambda \cdot T} \tag{34}$$

It follows that

$$\frac{dT}{T} = \frac{1}{n} \cdot \frac{dL_\lambda}{L_\lambda} \tag{35}$$

The typical range of values for $n$ is approximately $5 < n < 20$. The relative error in the measurement of emitted spectral radiance is thus seen to be reduced by a factor of $1/n$ in its effect on the relative error in the temperature. It is apparent that such errors can be minimized by maximizing $n$. This usually means using the shortest feasible wavelength, as in the case of window or emissivity effects, although there are circumstances (e.g., in the presence of reflected radiation) in which the opposite is true.

## CORRECTIONS FOR EMISSIVITY EFFECTS

If the emissivity is known and is essentially independent of wavelength across the radiometer passband, its effects can be compensated for by increasing the radiometer amplifier gain by a factor equal to the reciprocal of the emissivity. When the gain cannot be adjusted, as in the case of a disappearing-filament optical pyrometer or a null-balancing radiometer, a correction can be computed by substituting Wien's law into eq.(9), from which we obtain

$$\frac{1}{T} - \frac{1}{T_{apparent}} = \frac{\lambda}{c_2} \cdot \ln \varepsilon(\lambda) \qquad (36)$$

where $\lambda$ is the mean effective wavelength, discussed earlier. When the emissivity changes appreciably across the passband, we must use a different approach that is more direct but more

difficult to implement. The radiometer responds with the same signal that it would have if it were viewing a blackbody at the temperature $T_{apparent}$ From eq.(3Ø)

$$A_{n,d}\cdot\omega_d \cdot \int_0^\infty \mathcal{R}(\lambda)\cdot \tau(\lambda)\cdot\varepsilon(\lambda)\cdot L_{\lambda,b}(\lambda,T)\cdot d\lambda = A_{n,d}\cdot\omega_d\cdot \int_0^\infty \mathcal{R}(\lambda)\cdot\tau(\lambda)\cdot L_{\lambda,b}(\lambda,T_{apparent})\cdot d \quad (37)$$

The true temperature T is determined from the indicated temperature $T_{apparent}$ by numerical integration of the above expression. This requires numerical descriptions of $\varepsilon(\lambda)$, $\tau(\lambda)$ and $\mathcal{R}(\lambda)$. Prior to the advent of computers, this method - although exact in principle - required so much labor that it was seldom used. This no longer is true, although other methods may still be preferable in many cases, particularly for narrow passbands or where fast response is needed.

## RATIO THERMOMETERS

A ratio thermometer can be used to compensate for emissivity effects when the emissivity ratio $\varepsilon(\lambda_1)/\varepsilon(\lambda_2)$ is known. Such an instrument can be thought of as two nearly monochromatic radiometers operating at known wavelengths, $\lambda_1$ and $\lambda_2$ respectively, viewing the same target. From eq.(31),

$$S_1(T) = K_1\cdot\varepsilon(\lambda_1)\cdot L_{\lambda,b}(\lambda_1,T) \quad (38)$$

and

$$S_2(T) = K_2 \cdot \varepsilon(\lambda_2) \cdot L_{\lambda,b}(\lambda_2, T) \qquad (39)$$

where $K_1$ and $K_2$, or their ratio, are determined by calibration in terms of a blackbody or graybody From the ratio of the measured signals, and by substituting from Wien's law for $L_{\lambda,b}(\lambda, T)$, we have

$$R(T) = \frac{S_1(T)}{S_2(T)} = \frac{K_1}{K_2} \cdot \frac{\varepsilon(\lambda_1)}{\varepsilon\,\lambda_2} \cdot e^{-\frac{c_2}{T}\left(\frac{1}{\lambda_1} - \frac{1}{\lambda_2}\right)} \qquad (40)$$

which can be solved for the temperature, since all other quantities are known. This type of radiation thermometer is most frequently applied where graybody conditions have been shown to exist, i.e., where $\varepsilon(\lambda_1) = \varepsilon(\lambda_2)$, such as is often the case in the steel industry. Thus far, it has not proven satisfactory in aluminum industry applications because the spectral emissivity ratio at any two suitable wavelengths is too variable from one alloy to another. Ratio thermometers are also useful where only part of the target lies in the field of view, such as when dust obscures the target, or where the target is a hot wire passing through the field of view. It is only necessary that the same fraction of the field of view be used at each of the two wavelengths.

## FUTURE DEVELOPMENTS

Radiometric methods of temperature measurement have advanced to the point where commercially available radiometers operating in a number of spectral regions are widely used in industry, especially in process control and monitoring applications. While radiometer performance is presently satisfactory for most industrial applications, however, repeatability and noise levels often fall short of the mark required for research and development applications. The performance of a number of custom-built research radiometers, on the other hand, suggests that existing technology can support higher performance radiometry than is currently practiced in industrial radiation thermometry.

The effects of unknown emissivity and reflected extraneous radiation remain as the major hurdles for applied radiation thermometry, but the new hybrid methods are making serious inroads into these problem areas, and hold promise for much more progress. The development of hybrid methods was made possible, in turn, by the improved engineering understanding of the physics of thermal radiation from the surfaces of real materials and the development of related analytical techniques. The possibility of the widespread application of hybrid methods in the form of practical radiation thermometry

has been made likely to become reality by the recent advent of microprocessors.

These advances hold high promise for the development of methods and instrumentation that will greatly improve the accuracy and extend the range of application of radiometric methods. Future developments are likely to require a greater familiarity with the theory of radiometry and a detailed understanding of the radiative properties of surfaces.

## REFERENCES


1. Haugh, M.J., "Infrared Thermometry in the Aluminum Industry," Chapter 14 of "Theory and Practice of Radiation Thermometry," DeWitt, D.P., and Nutter, G.D., Editors, in publication.
2. DeWitt, D.P., "Thermal Radiative Properties - Metallic Elements and Alloys," Vol. 7, p. 28a, IFI Plenum, New York, 1970.
3. Porteus, J.O., "Relation Between the Height Distribution of a Rough Surface and the Reflectances at Normal Incidence," J. Opt. Soc. Am. 53, 1934-1402, 1963.

4. Touloukian, Y.S., and DeWitt, D.P., Ed., Thermophysical Properties of Matter, Vol. 7: "Thermal Radiative Properties, Metallic Elements and Alloys," Plenum Publishing Corp., New York (1970).

5. Reynolds, P.M., Brit. J. Appl. Physics, 12, 111-114 (1961).

6. Edwards, D.K., and Catton, I., from "Advances in Thermophysical Properties at Extreme Temperatures and Pressures," 3rd ASME Symposium on Thermophysical Properties, West Lafayette, Ind., 188-199 (1965).

7. Bennett, H.E., and Porteus, J.O., "Relationship Between Surface Roughness and Specular Reflectance at Normal Incidence," J. Opt. Soc. Am. 51, No. 2, 123-129, Feb., 1961.

8. Davies, H., "The Reflection of Electromagnetic Waves From a Rough Surface," Proc. Inst. Elec. Engrs. 101, 209-213, 1954.

9. Chinmayanandam, T.K., "On the Specular Reflection From Rough Surfaces," Phys. Rev. Vol. 13, 1919, p. 96.

10. Beckmann, P., and Spizzichino, A., "The Scattering of Electromagnetic Waves from Rough Surfaces," Macmillan, New York, 1963.

11. Blau, H.H. Jr., Marich, J.B., Martin, W.S., Jaspers, J.R., and Chafee, E., AFCRL-TR-60-416, 1-78, 1960 [AD 248276].

12. Research Projects Division, G.C. Marshall Space Flight Center, Huntsville, Ala., NASA-TN-D-1523, NASA-N63-14272, 1-253 (1963).

13. Bennet, J.M, and Bennett, H.E., "Polarization," Section 1Ø of Handbook of Optics, Driscoll, W.G., and Vaughan, W., (Ed.), McGraw Hill, New York, 1978.

14. Tingwald, C.P., and Magdeburg, H., "A New Optical Method for the Determination of Thermodynamic Temperatures of Glowing Metals, "Temperature, Its Measurement and Control in Science and Industry," Vol. 3, 483-486, Reinhold Publishing Corporation, New York, 1962.

15. Jenkins, F.A., and White, H.E., Fundamentals of Optics, Fourth Ed., McGraw Hill, New York, 1976.

16. Born, M., and Wolfe, E., Principles of Optics, Macmillan, New York, 1964.

17. Hess, G. and Waylonis, J.E., J. Opt. Soc. Am. 5Ø, 1133 (TB15) (196Ø).

18. Schulz, L.G., "The Optical Constants of Silver, Gold, Copper and Aluminum. I. The Absorption Coefficient k." J. Opt. Soc. Am. 44, 357 (1954). L.G. Schultz and F.R. Tangherlini, "Optical Constants of Silver, Gold, Copper and Aluminum. II. The Index of Refraction n". J. Opt. Soc. Am. 44 (1954).

19. Beattie, J.R., "The Anomalous Skin Effect and the Infrared Properties of Silver and Aluminum," Physica 23,

898 (1957). J. R. Beattie and G.K.T. Conn, Phil. Mag. 46, 989 (1955).

20. Gray, Dwight D., Ed., "American Institute of Physics Handbook," 3rd Edition, McGraw-Hill Book Co., New York (1972).

21. Lenham, A.P. and Treherne, D.M., "Optical Constants of Single Crystals of Mg, Zn, Cd, Al, Ga, In and White Sn," J. Opt. Soc. Am. 56, 752 (1966).

22. Bennett, H.E. and Bennett, J.M., "Validity of the Drude Theory for Silver, Gold, and Aluminum in the Infrared," in "Optical Properties and Electronic Structure of Metals and Alloys," F. Ables, Ed., p. 176. No. Holland Pub. (1966).

23. Siegel, R., and Howell, J.R., Thermal Radiation Heat Transfer, Second Ed., p. 104, Hemisphere Publishing Corp., McGraw Hill, New York, 1981.

24. Helmholtz, H. von, Handbuch der Physiologischen Optik, Third edition (Hamburg and Leipzig: Leopold Voss) pp 189-199 (1909).

25. Ref. [2], p. 32a.

26. Yates, H.W., and Taylor, J.H., "Infrared Transmission of the Atmosphere," U.S. Naval Research Laboratory, Washington, DC, NRL Report 5453, 1960.

27. Iuchi, T., and Kusaka, R., "Two methods for simultaneous measurement of temperature and emittance using multiple reflection and specular reflection, and their applica-

tions to industrial processes," Temperature, Its Measurement and Control in Science and Industry, Vol. 5, p. 491-503, American Institute of Physics, New York, 1982.

28. Kostkowski, H.J., and Lee, R.D., "Theory and Methods of Optical Pyrometry," Temperature, Its Measurement and Control in Science and Industry, Vol. 3, p. 449-481, Reinhold Publishing Corporation, New YHork, 1962.

29. Coates, P.B., "Wavelength Specifications in Optical and Photoelectric Pyrometry," Metrologia 13, 1-5, 1977.

30. Nutter, G.D., "Radiation Thermometers - Design Principles and Operating Characteristics," Chapter 4 of Theory and Practice of Radiation Thermometry," DeWitt, D.P., and Nutter, G.D., Editors, National Bureau of Standards, Washington, DC, in publication.

31. Zalewski, E.F., and Geist, J., "Silicon photodiode absolute spectral response self-calibration," Applied Optics, Vol. 19, No. 8, pp. 1214-1216, 15 Apr. 1980.